Numerical investigation of transient thermal and fluidynamic fields in an executive aircraft cabin

Vincenzo Bianco, Oronzio Manca, Sergio Nardini, Mario Roma

Accepted Manuscript

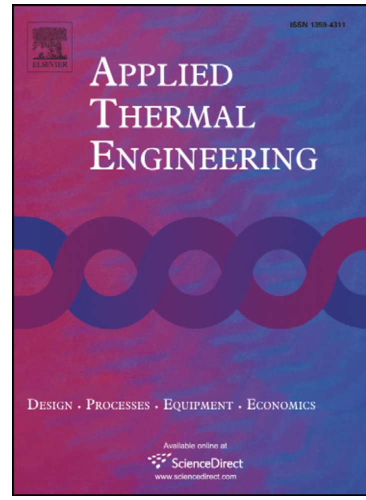

Numerical investigation of transient thermal and fluidynamic fields in an executive aircraft cabin

Vincenzo Bianco, Oronzio Manca, Sergio Nardini, Mario Roma

PII: S1359-4311(09)00173-2
DOI: 10.1016/j.applthermaleng.2009.05.020
Reference: ATE 2822

To appear in: *Applied Thermal Engineering*

Received Date: 16 January 2009
Revised Date: 27 April 2009
Accepted Date: 27 May 2009

Please cite this article as: V. Bianco, O. Manca, S. Nardini, M. Roma, Numerical investigation of transient thermal and fluidynamic fields in an executive aircraft cabin, *Applied Thermal Engineering* (2009), doi: 10.1016/j.applthermaleng.2009.05.020

NUMERICAL INVESTIGATION OF TRANSIENT THERMAL AND FLUIDYNAMIC FIELDS IN AN EXECUTIVE AIRCRAFT CABIN

Vincenzo Bianco[1], Oronzio Manca[1], Sergio Nardini[*,1], Mario Roma[2]

[1]DIAM – Seconda Università degli Studi di Napoli,

Via Roma 29, 81031 Aversa (CE) – ITALY

[2]Piaggio Aero Industries SpA,

Via Campi Flegrei 34, 80078 Pozzuoli (NA) – ITALY

Abstract

The objective of the present work is the numerical simulation of the thermal and fluid dynamic field in the cabin of an executive aircraft. A transient analysis is conducted on three and two-dimensional models of an executive aircraft cabin and a comparison of the two approaches is provided. In the model, a global thermal conductance was considered to take into account both the external environment and the fuselage material. The results, provided in terms of graphs and contours, refer to the three and two-dimensional models with inclined top inlets with respect to the vertical direction of an angle of 45°. A good

*Corresponding author: Tel.: +39 081 5010 347; fax: +39 081 5010 204
E-mail address: sergio.nardini@unina2.it (S. Nardini)

qualitative agreement between the results of the two and three dimensional models is detected.

Keywords: Airflow, aircraft air conditioning, CFD simulation, aircraft cabin, executive aircraft.

Nomenclature

A	Lateral area of the elementary cell, m^2
Cp	Specific heat of the fluid, J/(kg K)
g	Acceleration due to the gravity, m/s^2
k	Thermal conductivity, W/(m K)
L	Length of the elementary cell, m
p	Pressure, Pa
q	Heat flux, W/m^2
r	radius, m
R	Thermal resistance, K/W
t	Time, s
T	Temperature, K
U	Thermal conductance, $W/(m^2 K)$
V, v	Velocity, m/s
x	Horizontal coordinate, m
y	Vertical coordinate, m
z	Longitudinal coordinate, m

Greek letters

ρ Density, kg/m^3

τ Shear stress, N/m^2

Subscripts

avg Average

ext External

int Internal

T Turbulent

x Horizontal direction

y Vertical direction

z Longitudinal direction

1.0 Introduction

The reaction airplanes must fly to high altitude to furnish, in terms of fuel economy, the best performances. High altitudes are convenient in relationship to the fuel consumptions, but the same cannot be said for the external atmospheric conditions, that necessitate an isolation of the aircraft occupants from the external environment, characterized by low values of pressure and temperature. At an altitude of 11.000 m the air temperature is about -55 °C; the pressure is about one fifth of that with respect to the sea level and the damp is around zero. A system of environmental control is used for protection of passengers and crew in an aircraft from such extreme environmental conditions. The air distribution system is a fundamental component of the environmental control system of an aircraft because it should correctly distribute the conditioned air in the cabin, in order to realize a comfortable environment.

Higher occupant density, complex geometry and a lower supply of air rate per person when compared to buildings, make the design of a comfortable and healthy cabin environment for airplanes, especially for the executive class where top performances are required, very challenging.

In the last fifteen years, many numerical and experimental studies have been carried out, because of the importance of correct air distribution in the cabin. Mo et al. [1] used the Particle Image Velocimetry (PIV) to measure the distribution of air in the cabin of an aircraft in the absence of seats. Dechow [2] and Waters et al. [3] studied the air quality in the cabin measuring the quantity of contaminants, particulate and the concentration of ozone without studying the distribution of the air in detail. Garner et al. [4] conducted a campaign of measure in a Boeing 747 through two ultrasounds anemometers in absence of thermal loads and under conditions of static regime. Lately, Sun et al. [5] and Zhang et al. [6] performed experimental measures through velocimetry with a tide of particles in a Boeing 767-300 in presence of manikins. Recently, Kuhn et al. [7] experimentally investigated forced and mixed convection in a full scale passenger aircraft cabin mock-up. Large scale particle image velocimetry (PIV) and temperature field measurements were conducted in a cross sectional plane of the mock-up. Their study demonstrates that the flow field in aircraft cabins is affected by various fluid mechanical phenomena, such as interaction between the supplied air jets, buoyancy forces and thermal plumes interactions. All these parameters influence the flow field inside the cabin.

In comparison to the experimental investigations, the numerical ones are less expensive and it is possible to simulate situations similar to the reality, particularly for the transient state. This is especially true for medium size firms which produce executive aircrafts, because it would not be economically viable for them to build a mock-up in an environmental chamber and engage an expert experimental team to perform wide experimental analysis on the environmental control system. Otherwise, for this class of aircraft, the best performances are required, thus the CFD represents a very powerful tool to improve design and performances. For these reasons, in the last ten years, many numerical studies have been published. Aboosaidi et al. [8] were among the first to use the CFD to study the air distribution in the cabin of a commercial aircraft without passengers and thermal loads. A similar study was conducted by Mizuno and Warfield [9] who also appraised the concentration of carbon dioxide. To take into account the presence of the passengers, Singh et al. [10] used some heated cylinders placed on the seats.

A section of the Boeing 767-300 was recently investigated by Lin et al. [11, 12] using both the LES (Large Eddy Simulation) and RANS (Reynolds-average Navier-Stokes) models. Lately Zhang and Chen [13] used FLUENT with a RNG (Renormalization Group) k - ε model to study the distribution of the air flow, temperature and the concentration of the CO_2 in a section of a commercial aircraft with different kinds of distributions. Bianco et al. [14] investigated a two dimensional transient model of an aircraft section either with top inlets placed on the sides at an inclination of 45° with respect to the vertical or with top inlets placed in the middle section of the fuselage. The results show two vortex cells inside the cabin in both cases, that are unstable in the first case whereas they are stable in the second one.

Yan et al [15] presented a study on the airborne pollutant transport within an aircraft cabin mock-up with both experimental and CFD approach. A steady airflow field was simulated first and then it was compared with the experimental data. The study demonstrated how

CFD simulations can help to understand the pollutant transport mechanism. They provide more detailed information, which cannot be exclusively obtained by experiments.
Recently Zhang et al. [16] investigated airflow and contaminant transport in an occupied cabin by both experimental measurements and numerical simulation with CFD. The numerical simulation used the Reynolds averaged Navier-Stokes equations based on the RNG k- ε model to calculate the air velocity, air temperature and concentration of gas contaminants. Their numerical results quantitatively agreed with the experimental data whereas some remarkable differences exist in airflow distribution.
Most papers present in the literature focus on the CFD airflow simulation and experimental investigation in large passenger aircraft cabins. The aim of the authors is to cover the lack of information regarding the executive class.
The purpose of the present work is the numerical visualization of the thermal and fluid dynamic field in the cabin of an executive aircraft, in order to collect information to improve the air conditioning design. A transient analysis is conducted on two and three dimensional models of the aircraft cabin and a comparison of the two approaches is performed, in order to estimate the trade off between accuracy and velocity of the solution.
In the model, a global thermal conductance is estimated and assigned to take into account both the external environment and the fuselage material. The results refer to the two and three dimensional models with the top inlets inclined with respect to the vertical axis of an angle of 45°. To the authors best knowledge, this represents the first paper which focuses specifically on this special class of aircraft.
It is important to remark that the present analysis is not completely able to capture the effects due to passengers and seats as well as the effect of a different overheads inclination.

2.0 Numerical model

2.1 Governing equations

The problem under investigation is a two and three dimensional simulation of an executive aircraft cabin in transient mixed convection. The transient problem was solved by the commercial code FLUENT 6.2 [17].

The flow is assumed incompressible and, depending on the model considered, two or three dimensional, a turbulence model is, however, used to take into account the viscous effects. In the following equations, "D/Dt" is the material derivative and the symbol " ¯ " refers to time averaged quantities.

$$\nabla \cdot \overline{V} = 0 \qquad (1)$$

$$\rho \frac{D\overline{V}}{Dt} = -\nabla p + \rho(T) \cdot g + \nabla \cdot \left(\tau - \tau_T\right) \qquad (2)$$

$$\rho Cp \frac{D\overline{T}}{Dt} = \nabla \cdot \left(q - q_T\right) \qquad (3)$$

The governing equations of the fluid flow (1-3) constitute a highly non-linear and coupled partial differential equations system. In fact the density, ρ, is linked to energy equation being a temperature function. The well known Boussinesq approximation is considered to take into account temperature dependence of density.

The resulting equations system should be solved taking into account appropriate boundary conditions; and since the problem is turbulent, closure equations are required to arrive at the solution. Empirical data or approximate models are required to express the turbulent stresses and heat flux quantities of the related physical phenomenon.

In the present analysis, $k - \varepsilon$ turbulent model in the RNG form is adopted, because it was broadly validated by other authors in different enclosed environments [13,16,18-20] and, moreover, for the case analyzed in the present paper, to the best of our knowledge, experimental data, to validate the model, do not exist.

2.2 Boundary and initial conditions

For the considered aircraft section, inlet air velocity and temperature were fixed; the position of outlet sections was assigned and wall conductance and external temperature were assigned on the walls.

From the right and left overheads (Fig. 1), placed in the top part of the cabin, air is introduced at a velocity of 6.0 m/s and at a temperature of 318 K, while from the right and left side diffusers, positioned in the lower part of cabin, air is introduced at a speed equal to 0.4 m/s and at a temperature of 318 K. The air is expelled to the outside through the outlets corresponding to the corridor.

The other surfaces are walls subjected to convection at a temperature of 245 K with an imposed average conductance equal to 3 W/(m^2K). The two closure faces are considered symmetrical surfaces, hence the derivatives of all the quantities are equal to zero.

In the case of the two-dimensional approximation, in order to balance the non perfect longitudinal symmetry, a lower inlet air temperature, equal to300 K, was considered. The two overheads in the 2D model were considered like a "strip" injection over all the longitudinal length, while in reality they are two punctual air injections, such that the quantity of hot air supplied to the cabin is higher. To avoid an over heating effect, the temperature is lowered.

The criteria used is to work with constant enthalpy, so that if the air flow rate is higher (strip injections), to balance the enthalpy, the air temperature is lowered. In this way, it is possible to obtain a 2D model which gives a good qualitative approximation of the 3D model, as will be shown in the results.

A time step of 0.1 s is adopted for the transient calculation and it was chosen in order to guarantee the solution convergence.

Initially the air inside the cabin is calm at a temperature equal to 295 K. At t=0 s, the air enters into the cabin through two overheads positioned in correspondence of passengers head, inclined of 45° in comparison to the vertical and from two side diffusers placed in proximity of the passengers feet.

The fuselage is composed of various materials assembled in parallel/series. Particularly, there are: "Microlite 0.4" and "Microlite 0.6" placed in series and both are parallel, with an aluminium frame, which has a structural function, as shown in Fig. 1c.

A further complication to the aforementioned problem has to do with the fact that aluminium and microlite conductivities differ by four magnitude orders, hence a simple series-parallel model is not applicable since the temperature field is not one-dimensional, but two-dimensional [21].

In order to calculate an average conductivity for aluminium, "Microlite 0.4" and "Microlite 0.6" (Fig. 1c), a finite volume numerical model was implemented. The model consists of a rectangular domain, composed by the aforementioned materials (as reported in Fig. 1c), and in two assigned temperatures imposed on the vertical sides, one cold and the other hot, with adiabatic horizontal sides. The average heat flux was determined by means of the numerical model and, consequently, the average thermal conductivity was calculated. The estimated value for the thermal conductivity (k_{avg}) is 0.16 W/(mK).

Once the average conductivity is estimated, it is possible to calculate the average conductance, which represents the parameter to impose in the aircraft cabin model.

In order to do this, the fuselage is considered as a hollow cylinder with length equal to the length of the elementary cell, Fig. 1c, composed of a part in aluminium and another in microlite, repeating itself in the space. The following equation is used to calculate the thermal resistance:

$$R = \frac{\ln \frac{r_{ext}}{r_{\text{int}}}}{2 \cdot \pi \cdot L \cdot k_{avg}} \qquad (4)$$

where r_{ext} and r_{int} are equal to 0.96 m and 0.91 m respectively (Fig. 1c and 2a), whereas L is equal to 0.185 m (Fig. 1c). Once the thermal resistance is obtained, the conductance can be calculated by making the reciprocal of R and dividing this value by the lateral area of the elementary cell:

$$A = 2 \cdot r_{ext} \cdot L \qquad (5)$$

This estimated conductance value, U, is equal to 3.0 W/(m^{2}K).

2.3 Geometrical modelling and grid generation

The transient numerical investigation was carried out on two and three dimensional model of a section of an executive aircraft cabin. In this first study, the cabin was considered void, without taking seats and passengers into account.

The transversal section of the aircraft, shown in Fig.1a and 2a, was modelled using Gambit [17] and to obtain the three-dimensional model, it was extruded by 1237 mm along the longitudinal axis, Fig. 1b and 2b.

Treated air enters the aircraft cabin from 4 inlets: two inlets on the top in proximity of the passengers head, inclined at an angle of 45° with respect to the vertical direction and two side diffusers in proximity of the passengers feet.

The computational grid was built using tetra elements, refined in proximity of the air inlets and outlets sections. The skew value is considered in order to measure the mesh quality; it varies between 0 and 1 and it should be the lowest possible in order to build a model that guarantees the convergence.

A grid independence analysis has been performed and, for this reason, different grids are tested. The mesh that introduces acceptable errors, with respect to the most refined grid tested, was selected in order to arrive at a correct compromise between time of calculation and accuracy of the results. The accuracy control parameter of the results was the transient average temperature on the cabin wall "Wall 1", Fig. 1b and Fig. 3.

The selected grid is the medium one, which is composed of 476.073 cells and introduces a maximum value of skewness equal to 0.75, while the difference in terms of medium temperature, expressed in degrees Celsius, with respect to the fine grid is about 5%, as reported in Fig. 3.

2.4 Numerical method

The system of governing equations, subject to their appropriate boundary conditions, was successfully solved by using the finite volume method. This method is based on the spatial integration of the conservation equations over finite control volumes for each time step, converting the governing equations to a set of algebraic equations.

The algebraic "discretized equations" resulting from this spatial integration process were sequentially solved throughout the physical and temporal domain considered. The computational analysis was performed by employing the commercial software FLUENT. Conservation equations residuals are considered as convergence indicator and they were set in the following way: 10^{-3} for mass conservation, 10^{-4} for momentum equation and 10^{-6} for energy conservation. During the iterative process the residuals were carefully monitored and the convergence was checked for each time step.

The solution was obtained on a XEON with two 32 bit processor of 2.40 GHz each and 2GB of RAM. It took about five days to simulate 800s.

3.0 Results

Results are presented in terms of velocity and temperature for two and three dimensional transient simulations. The quasi steady state in the case of three dimensional model is achieved after about 500 s, as shown in Fig. 3, while for the two dimensional model after about 30 s, as reported in Fig. 4b. The oscillating behaviour shown in Fig. 3 is due to the presence of vortex inside the cabin, as subsequently explained. The oscillations remain and the motion is therefore considered as quasi steady state.

3.1 Two-dimensional model results

For the two dimensional model, Fig. 4a shows the vertical component of velocity, v_y, as a function of the horizontal coordinate for different times. The profiles are characterized by oscillation during the time. In fact, the absolute minimum continuously changes its position along the profile. This is due to the reciprocal impact of the two warm air jets coming from the overheads. One of them alternatively predominates on the other, such that one is recalled on the upper part of the cabin provoking a recirculation zone, while the other is able to penetrate deeper in the cabin, causing the main vortex. This oscillation causes the instability of the two main vortexes inside the cabin, as shown in Fig. 5. This behaviour is more pronounced in the two dimensional model, because the longitudinal direction is neglected. In the subsequent three dimensional model, it is possible to notice that the longitudinal dimension plays a part in limiting this phenomenon as the jets dissipate their energy longitudinally.

Fig. 4b shows that a quasi steady state, for the two dimensional case, is achieved after about 30 s. In fact, the temperature profiles at 60 s, 90 s and 120 s are practically overlapped. Moreover, a slight increase of temperature along the profiles is detected in correspondence to maximum velocity magnitude. This happens in one fourth of the cabin width in central part of the section, as highlighted by the shaded areas of Fig. 4a and 4b. Temperature is quite uniform inside the cabin, but there is a strong drop near the wall and probably one or more insulating substrates are required.

3.2 Three-dimensional model results

In Fig. 6a, temperature values for three dimensional model in overhead section along line 1, as a function of the time, are reported. Temperature decreases with time until the steady state around 500 s, as shown also in Fig. 3. The peak value, about 297 K close to the middle of the section, is due to the two jets which merge in this zone and then start to oscillate. In fact, the maximum value continuously changes its position. Moreover, considering the profiles at 600 s and 800 s, it is detected that, on the left of the maximum, for 600 s the temperature value is higher than the one for 800s, while on the right part, the opposite is observed. This is due to the left jet, at this time, which pushes the right one towards the cabin wall. This behaviour changes with time and consequently, temperature field is never symmetric, even if the geometry and boundary conditions are symmetric.

In Fig. 6b, temperature along line 1, for different sections at 800 s is given. In section 3, which is 0.089 m far from the overhead, the peak due to the jets is visible. The maximum value along the profile is attained at different points for different sections, as highlighted by the shaded area of Fig. 6b. It is concluded that there is jets oscillation also in the longitudinal direction, as clarified from the pathlines, which are omitted for the sake of brevity . However, the zone along the width is between about 0.7 m and 1.0 m. Temperature is almost uniform inside all the cabin, reaching the value of about 294 K, and this is very important in order to guarantee the passengers thermal comfort. A strong temperature drop is detected just on the cabin wall.

Temperature fields, omitted for sake of brevity, confirm that the temperature is rather uniform in all the section, just a warmer vortex is in the central upper part of the section, which moves alternatively due to the two warm jets coming from the overheads.

The horizontal component of velocity, for different time steps, is presented in Fig. 7a. It is possible to notice some peak values at y=0.4 m with a value of about 0.4 m/s, which represents the jet coming from the side diffuser. For t=600 s, this maximum velocity value is not present, probably due to the vortex on the left side of the cabin which recalls the jet coming from the left side diffuser. Fig. 7b shows the horizontal velocity component at t=800 s along different sections. A peak in section 2, in the lower part of the cabin, is observed. This is due to the warm air jet coming from the left side diffuser, while in section 3, there is a peak value in the upper part of the cabin, which is probably due to overhead jets oscillation along the longitudinal plane, in agreement with Fig. 6b, where, in the same section, the maximum is detected. As for the other sections, it is possible to notice velocity fluctuations, probably due to the flow field instability, which is caused by the vortex movements. This guarantees a uniform temperature in order to ensure passenger comfort. On the contrary, fluctuating velocity may determine discomfort conditions in the cabin.

In Fig. 7c, the vertical velocity component, for different times, is reported. The figure shows a minimum, which corresponds to the jets impact zone inside the cabin and fluctuations around x=0.8 m are observed at different times, as evidenced by the shaded area of Fig. 7c. On the left and on the right of the minimum point, the velocity alternatively increases and decreases. Particularly, when the minimum is placed on the left part of the section, the average velocity value on the right part is higher and vice versa. This oscillating effect is due to the impact of the two jets: one jet tends to push the other. When the minimum velocity value moves on the left, it means that the right jet is prevailing on the left one and the opposite is the case when the minimum velocity value moves on the right. The vertical velocity component at t=800 s is reported in Fig. 7d at different sections, where a minimum point at around x=0.8 m is observed, which corresponds to the jet penetration in the cabin. Moreover, this minimum point is present for section 2 and 3. This is due to the fact that the jets oscillate also in the longitudinal plane. In the other sections, the vertical velocity component results quite oscillating between -0.2 m/s and 0.1 m/s.

The flow oscillations inside the cabin are highlighted by the velocity vectors fields at different times in Fig. 8. At t=200s the two jets merge into a quasi symmetrical flow in the middle section and four macro vortex cells are detected, two in each side. The merged flow moves toward the right side at t=400s, Fig. 8a, and the lower vortex cell in the left side expands. This effect should determine a depression in the left zone and the right jet push the left jet toward the left side. The merged flow moves toward the left part of the section, as shown in Fig. 8b. At t=600s and 800s, the right side has a lower pressure and flow moves toward the right side. Therefore, a sort of flip-flop flow is detected inside the cabin. When the jets meet, they also expand along the longitudinal direction, giving room to a motion in this direction, as shown by means of the path lines coming from the overheads at different times, which are not reported for sake of brevity. These path lines show that the motion field is quite disordered and characterized by many fluctuations, which affect the comfort of the cabin occupants.

However, the presence of these various motion fields tend to generate a more uniform temperature field, because of the high mixing effect.

4.0 Conclusions

In the present paper, thermal and velocity fields, in a section of an executive aircraft, were numerically investigated. The transient behaviour of the cabin is analyzed on two and three-dimensional models and a global thermal conductance is considered to account for both the external environment and the fuselage materials.

Results of two-dimensional and three-dimensional models show a good qualitative agreement. In fact, all the main phenomena are predicted by the two dimensional model, irrespective of differences from the quantitative point of view. This is true, especially for the velocity field, that in the two dimensional model, does not consider the longitudinal direction and the kinetic energy is dissipated in a smaller domain, leading to higher values of the velocity. In terms of temperature the values are comparable because an enthalpy correction was adopted. It is important to remark that the indications given from the two dimensional model are very effective from a qualitative point of view, especially because they are immediately available. In fact, the numerical solution of a two dimensional model takes some minutes, while the three dimensional one takes some days. The aim is to perform a fast pre-optimization analysis on the two-dimensional model and then upgrade it to a three dimensional one.

Three dimensional model results outline that the thermal field seems adequate to guarantee the passengers comfort. In fact, there is an average temperature of about 294 K and just on the adjacent wall, there is a strong drop. Therefore, the wall insulation should be increased. On the other hand, the velocity values have a correct magnitude to provide comfort conditions. They are in the order of ± 0.1 m/s, except in proximity of the air inlets where they increase. However, they are characterized by fluctuations, which may cause passengers discomfort.

It is important to remark that, this is a first attempt to model thermal and velocity fields inside an executive aircraft cabin, therefore the presented results have limited practical application. Future improvement may be represented by the inclusion of seats and passengers, whose presence undoubtedly affect the flow configuration and by performing an optimization of the overheads inclination, in order to improve the significance of results.

References

[1] H. Mo, M. Hosni, B. Jones, Application of particle image velocimetry for the measurement of the airflow characteristics in an aircraft cabin, ASHRAE Transactions 109 (2003) 101–110.

[2] M. Dechow, Concentrations of selected contaminants in cabin air of airbus aircrafts, Chemosphere 35 (1997) 21–31.

[3] M. Waters, T. Bloom, B. Grajewski, Measurements of indoor air quality on commercial transport aircraft, Proceedings of Indoor Air (2002) 782–787.

[4] R. Garner, K. Wong, S. Ericson, CFD validation for contaminant transport in aircraft cabin ventilation flow fields, Proceedings of annual SAFE symposium. Survival and flight equipment association (2003) 248–53.

[5] Y. Sun, Y. Zhang, A. Wang, J. Topmiller, J. Bennett, Experimental characterization of airflows in aircraft cabins, Part 1, Experimental system and measurement procedure. ASHRAE Transactions 111 (2005) 45–52.

[6] Y. Zhang, Y. Sun, A. Wang, J. Topmiller, J. Bennett, Experimental characterization of airflows in aircraft cabins, Part 2, Results and research recommendations. ASHRAE Transactions 111 (2005) 53-59.

[7] M. Kuhn, J. Bosbach, C. Wagner, Experimental parametric study of forced and mixed convection in a passenger aircraft cabin mock-up, Building and Environment doi:10.1016/j.buildenv.2008.06.020

[8] F. Aboosaidi, M. Warfield, D. Choudhury, Computational fluid dynamics applications in airplane cabin ventilation system design, Proceedings of Society of Automotive Engineers 246 (1991) 249–58.

[9] T. Mizuno, M. Warfield, Development of three dimensional thermal, airflow analysis computer program and verification test, ASHRAE Transactions 98 (1992) 329–38.

[10] A. Singh, M. Hosni, R. Horstman, Numerical simulation of airflow in an aircraft cabin section, ASHRAE Transactions 108 (2002) 1005–1013.

[11] C. Lin, R. Horstman, M. Ahlers, L. Sedgwick, K. Dunn, J. Topmiller et al. , Numerical simulation of airflow and airborne pathogen transport in aircraft cabins—Part 1, Numerical simulation of the flow field, ASHRAE Transactions 111 (2005) 755–763.

[12] C. Lin, R. Horstman, M. Ahlers, L. Sedgwick, K. Dunn, J. Topmiller et al. , Numerical simulation of airflow and airborne pathogen transport in aircraft cabins—Part 2: Numerical simulation airborne pathogen transport, ASHRAE Transactions 111 (2005) 764–768.

[13] T. Zhang, Q. Chen, Novel air distribution systems for commercial aircraft cabins, Building and Environment 42 (2007) 1675-1684.

[14] V. Bianco, B. Buonomo, O. Manca, S. Nardini, Analisi termofluidodinamica bidimensionale della climatizzazione di un aeromobile, Proceedings XXV Congresso della Trasmissione del Calore UIT, Trieste 2007.

[15] W. Yan, Y. Zhang, Y. Sun, D. Li, Experimental and CFD study of unsteady airborne pollutant transport within an aircraft cabin mock-up, Building and Environment 44 (2008) 34-43.

[16] Z. Zhang, X. Chen, S. Mazumdar, T. Zhang, Q. Chen, Experimental and numerical investigation of airflow and contaminant transport in an airliner cabin mockup, Building and Environment 44 (2009) 85-94.

[17] Fluent Incorporated, Fluent 6.2, User Manual, 2006.

[18] Q. Chen, Z. Zhang, W. Zuo, Computational fluid dynamics for indoor environment modeling: past, present and future. Proceedings XXV Congresso della Trasmissione del Calore UIT, Trieste 2007.

[19] Q. Chen, Comparison of different k – ε models for indoor air flow computations. Numerical Heat Transfer, Part B 28 (1995) 353-369.

[20] Z. Zhang, W. Zhang, J. Z. Zhai, Q. Chen, Evaluation of various turbulence models in predicting airflow and turbulence in enclosed environments by CFD. Part-2: Comparison with experimental data from literature. HVAC&R Research 13 (2007) 871-886.

[21] F. P. Incropera, D. P. DeWitt, Fundamentals of Heat Transfer, John Wiley & Sons, New York, 1995.

Figure Captions:

Figure 1: (a) Two dimensional domain, (b) Three dimensional domain and (c) Schematic representation of fuselage composition. The sketched "cell" repeats itself in the space.

Figure 2: (a) References lines "Position 1" (P1) and "Line 1" (L1) for velocity and temperature plots and (b) Cabin sections (S1, S2, S3, S4) for results analysis.

Figure 3: Average transient temperature on "Wall 1" used to assess grid independence.

Figure 4: Velocity and temperature profiles for 2D model along line 1: (a) transient velocity vertical component and (b) transient temperature, for different times, 10, 30, 60, 90 and 120 s.

Figure 5: Stream function fields in 2D model after: (a) 30s and (b) 60s.

Figure 6: Temperature profiles in 3D model: (a) transient temperature behaviour in the section 2 along line 1 at different time values and (b) temperature at t=800 s in different sections along line 1.

Figure 7: Horizontal velocity component along position 1 (a) in section 2 at different time steps and (b) at t=800s for the different sections. Vertical velocity component along the line 1: (c) in section 2 for different times and (d) at t=800s for the different sections.

Figure 8: Velocity field in section 2 at different times (a) t=400 s and (b) t=800 s.

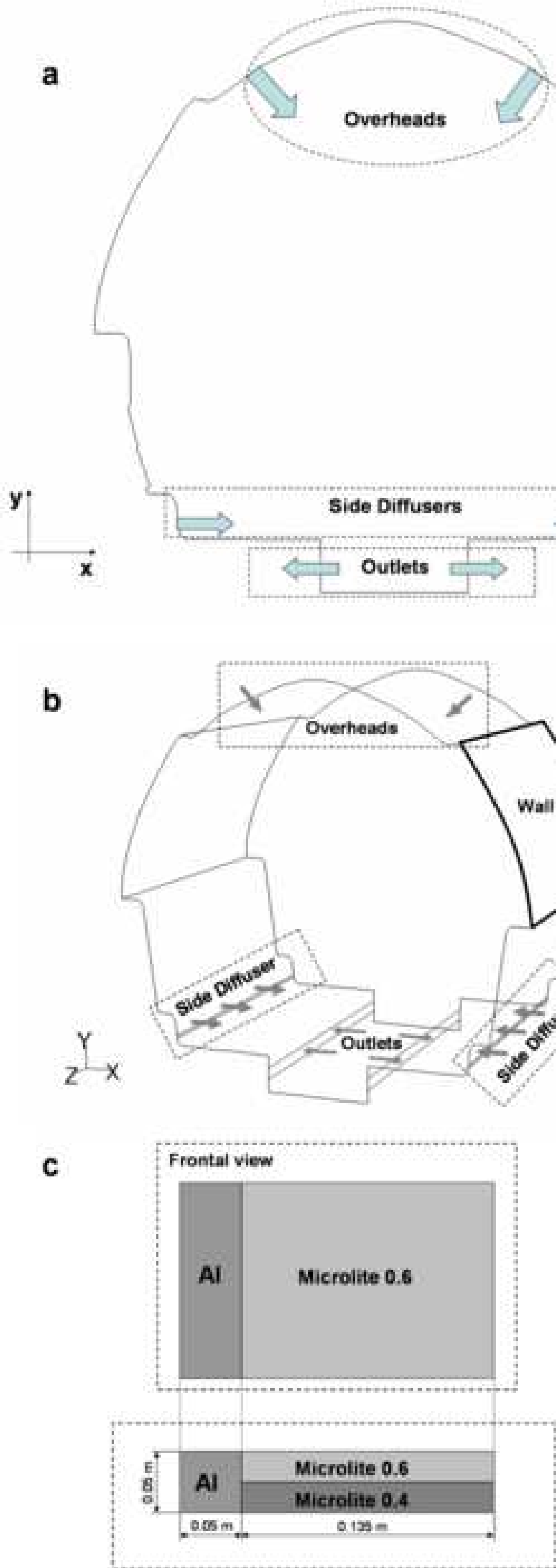

a
Overheads
Side Diffusers
Outlets
y
x
b
Overheads
Wall 1
Side Diffuser
Outlets
Side Diffuser
Y
Z
X
c
Frontal view
Al
Microlite 0.6
Al
Microlite 0.6
Microlite 0.4
0.05 m
0.05 m
0.135 m

a

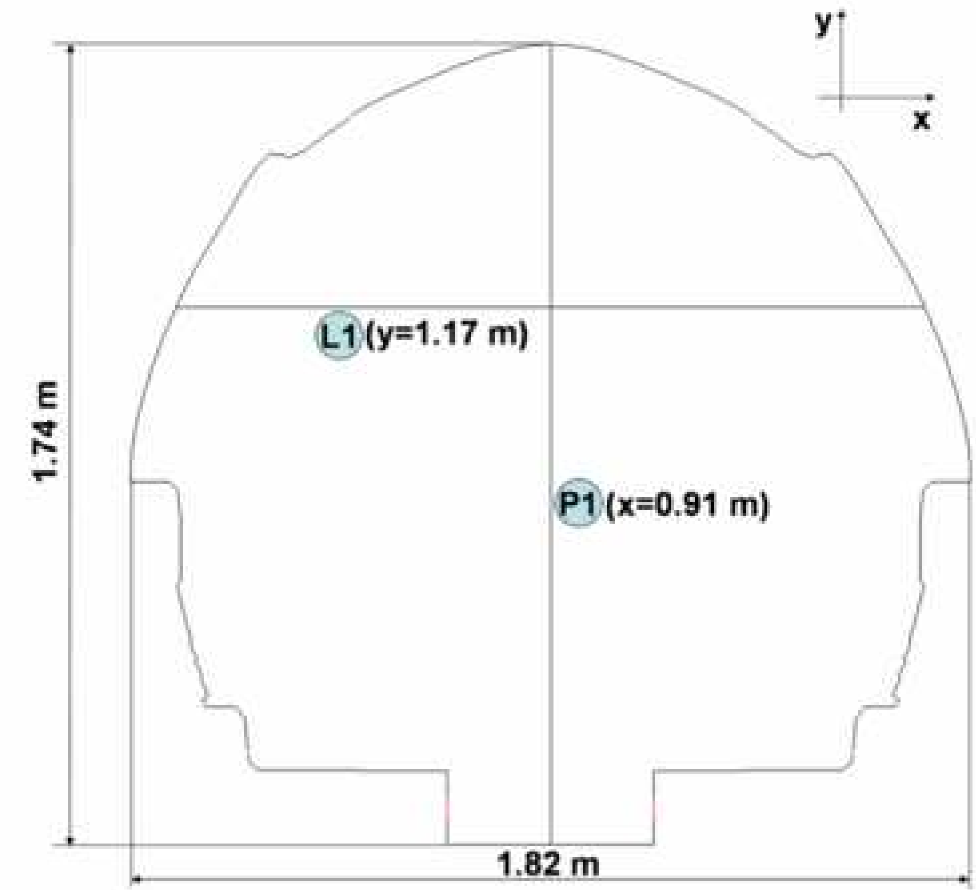

b

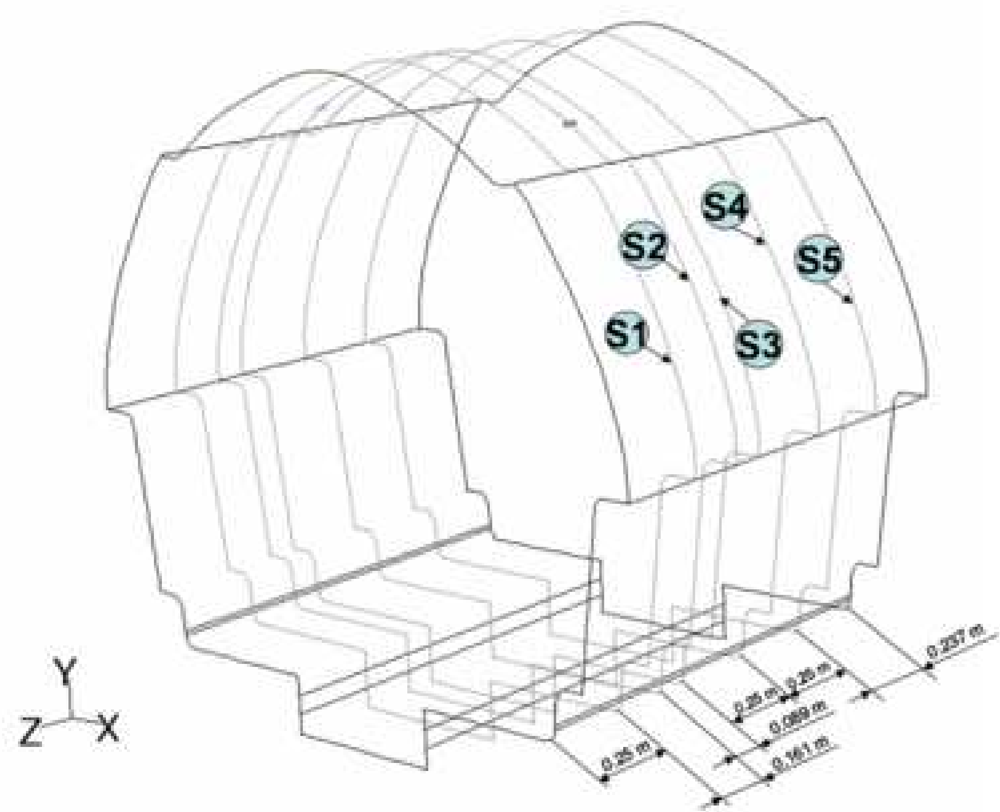

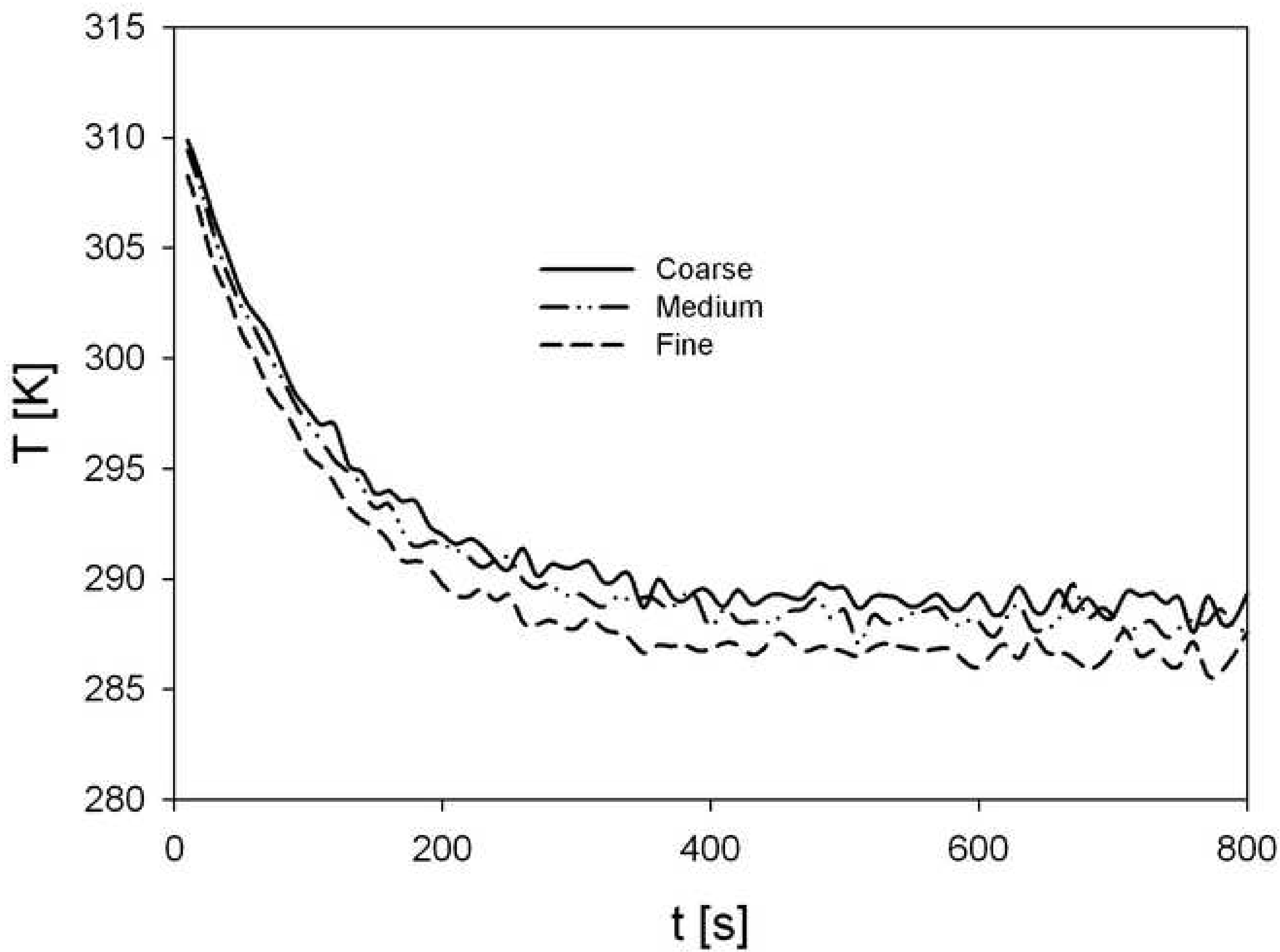
T [K]
t [s]
Coarse
Medium
Fine
315
310
305
300
295
290
285
280
0
200
400
600
800

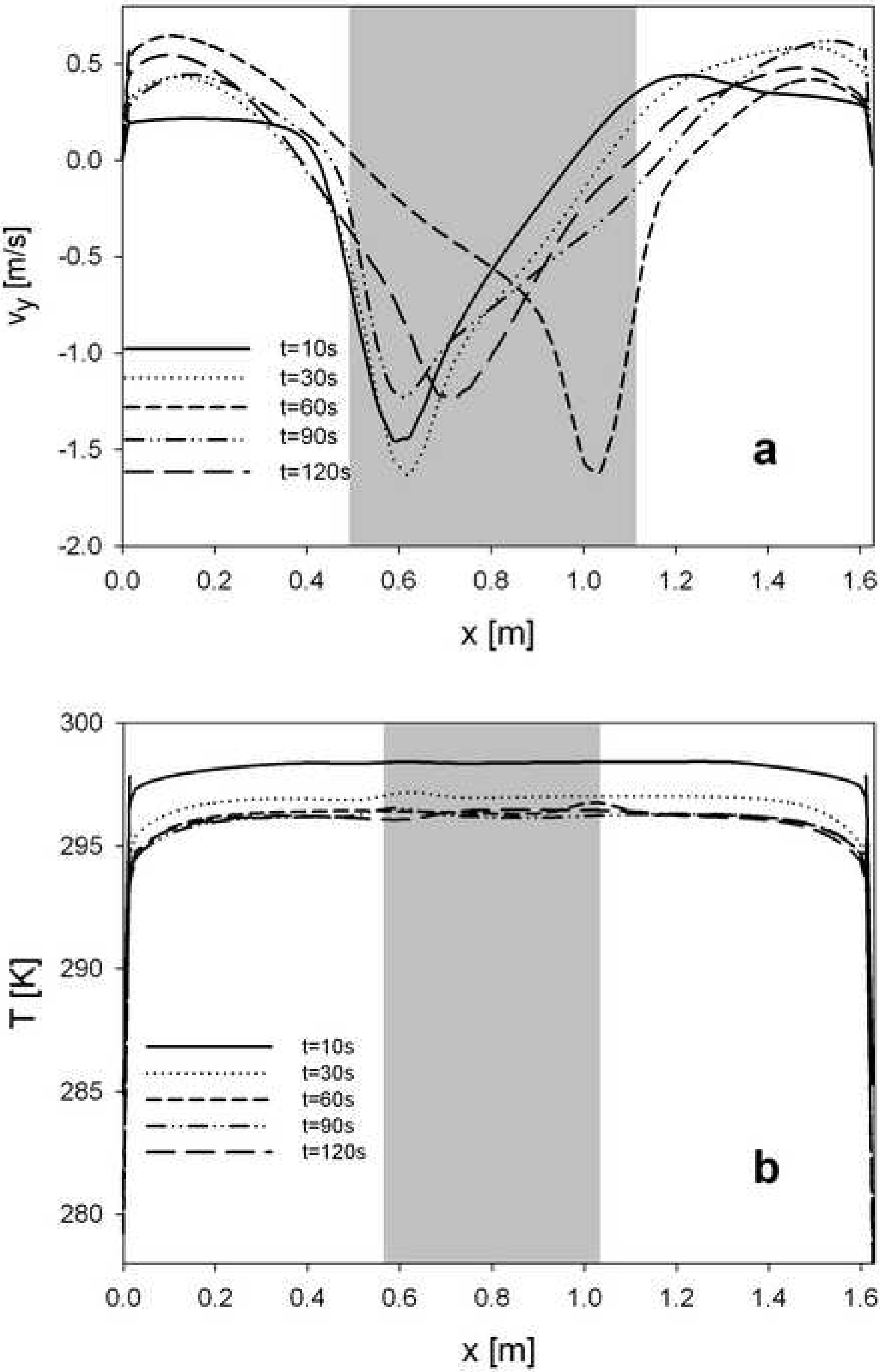

0.5
0.0
-0.5
-1.0
-1.5
-2.0
v_y [m/s]
t=10s
t=30s
t=60s
t=90s
t=120s
a
0.0
0.2
0.4
0.6
0.8
1.0
1.2
1.4
1.6
x [m]
300
295
290
285
280
T [K]
t=10s
t=30s
t=60s
t=90s
t=120s
b
0.0
0.2
0.4
0.6
0.8
1.0
1.2
1.4
1.6
x [m]

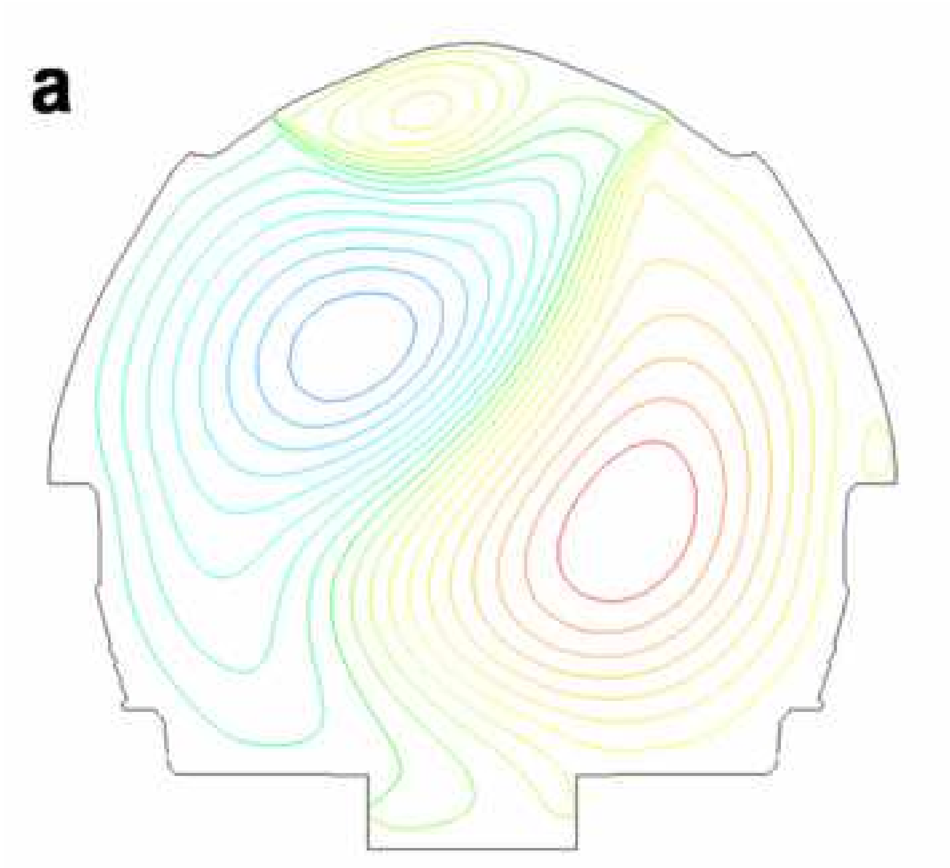

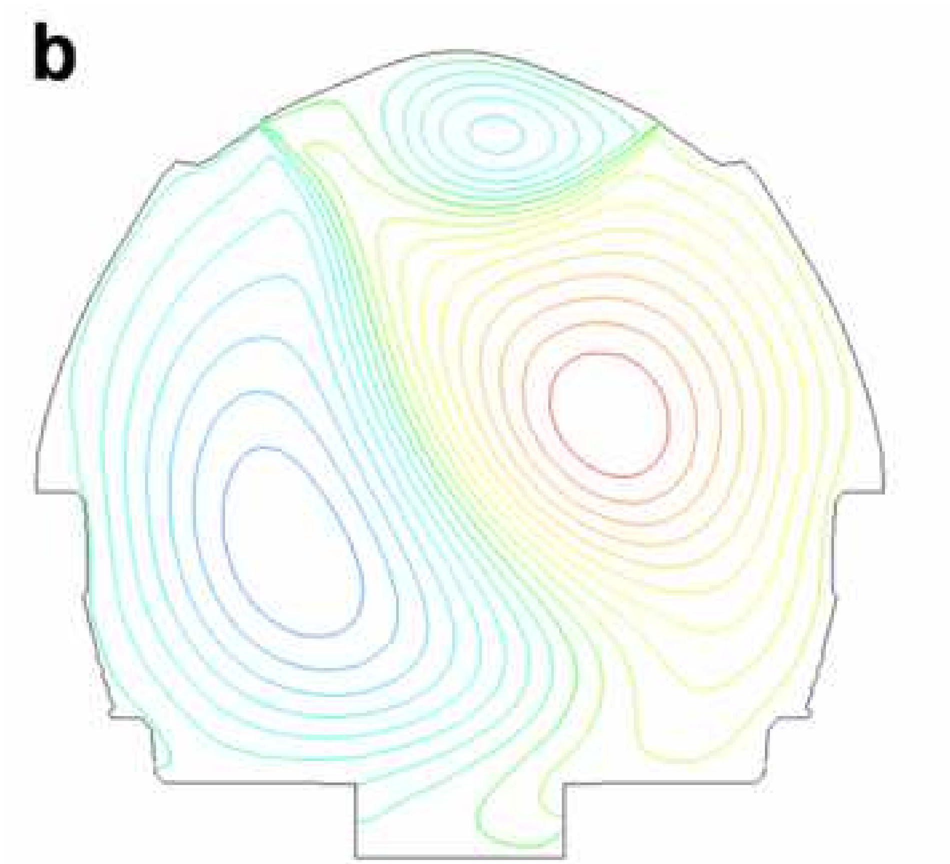

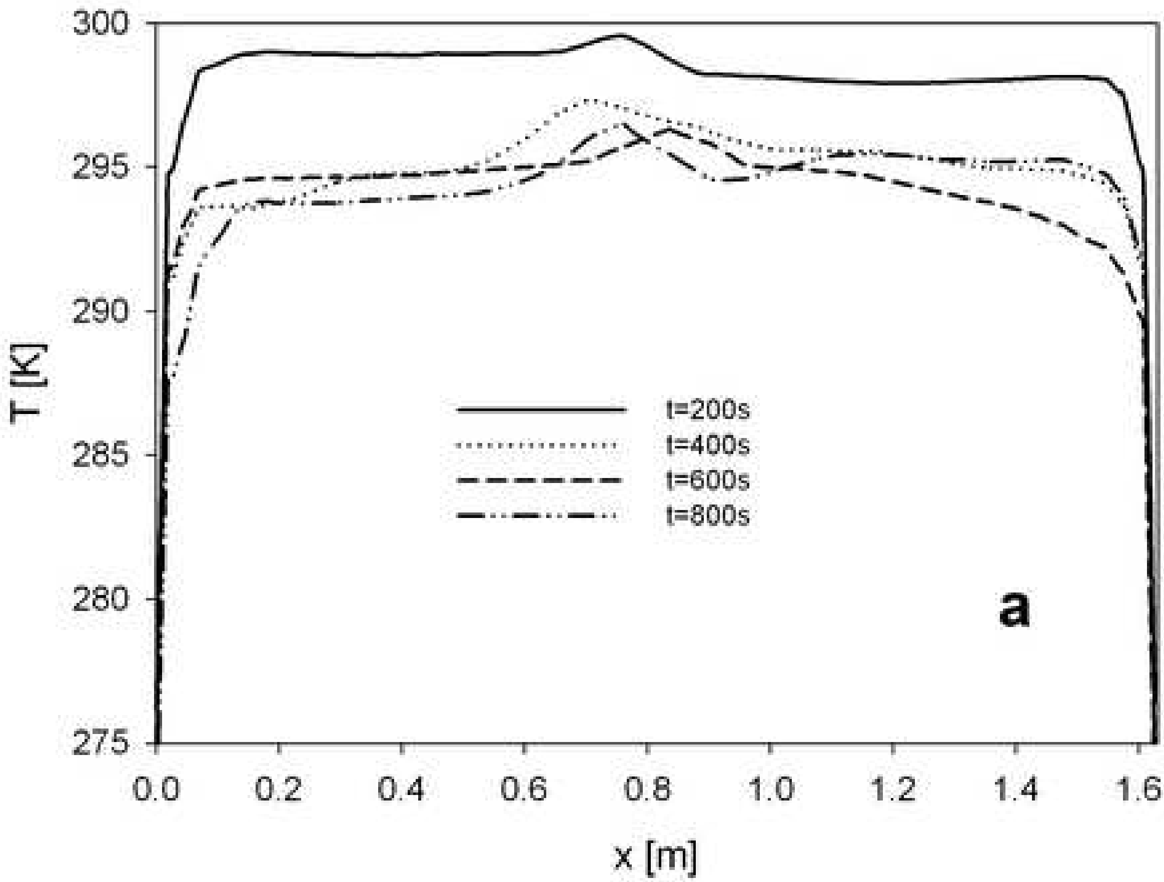
300
295
290
285
280
275
T [K]
0.0
0.2
0.4
0.6
0.8
1.0
1.2
1.4
1.6
x [m]
t=200s
t=400s
t=600s
t=800s
a

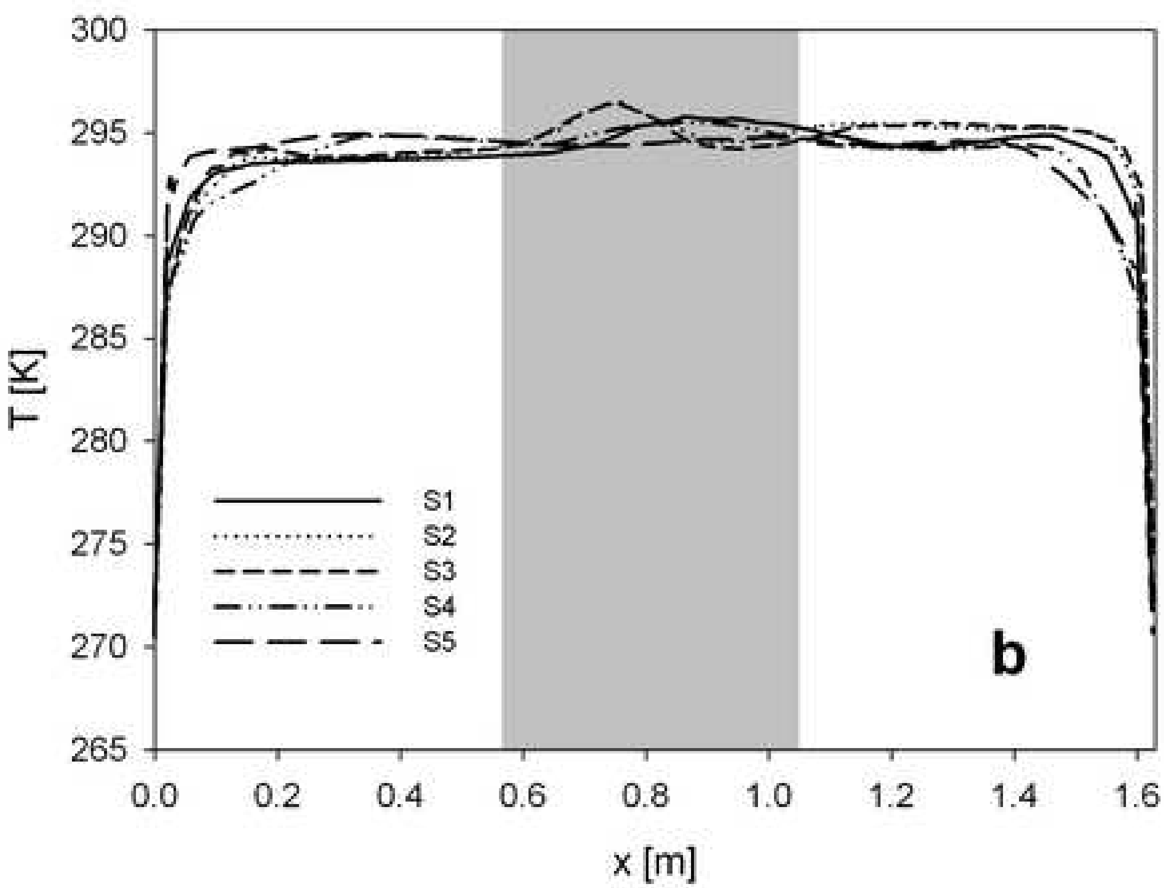
300
295
290
285
280
275
270
265
T [K]
0.0
0.2
0.4
0.6
0.8
1.0
1.2
1.4
1.6
x [m]
S1
S2
S3
S4
S5
b

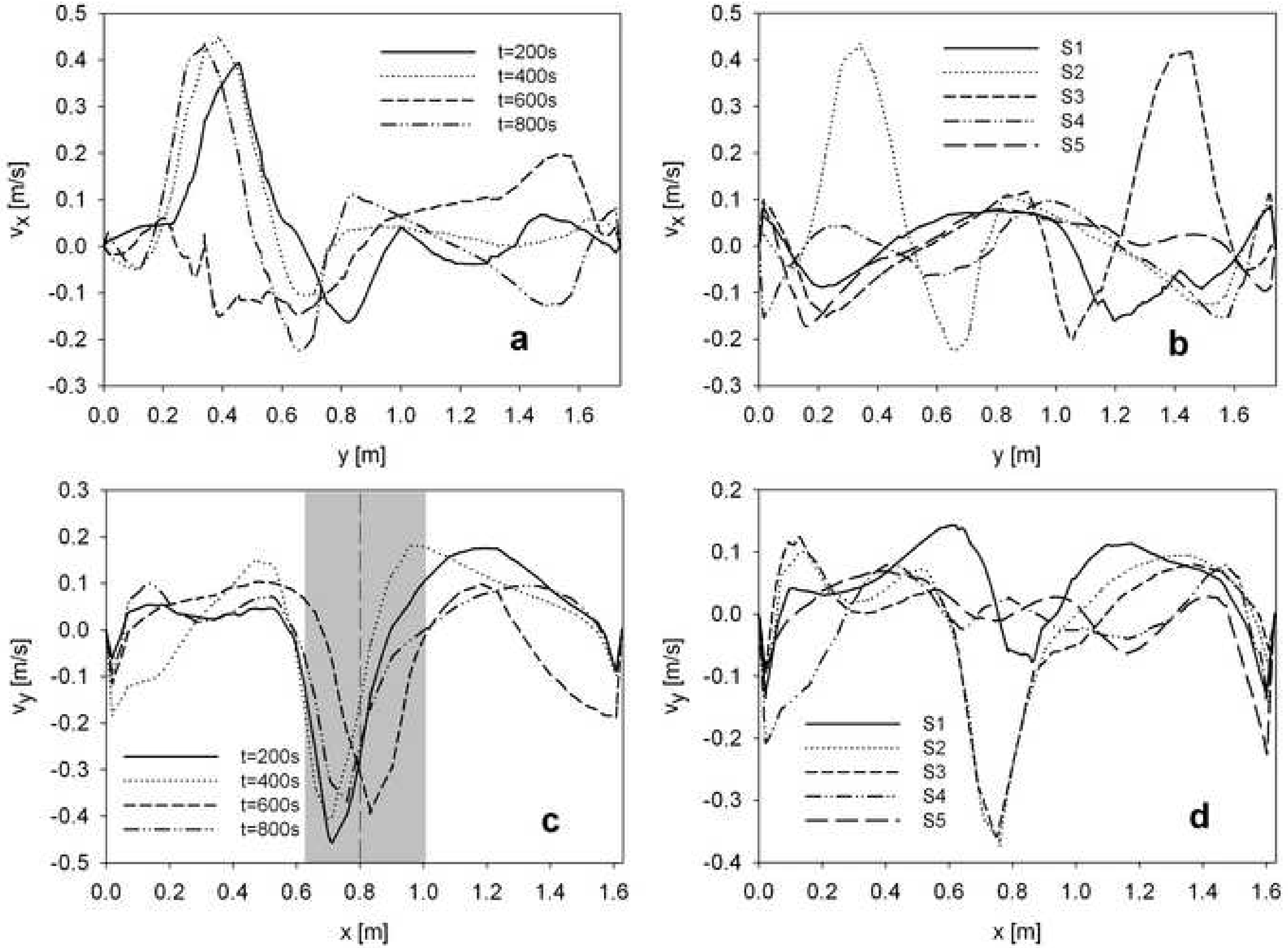
0.5
0.4
0.3
0.2
0.1
0.0
-0.1
-0.2
-0.3
vx [m/s]
t=200s
t=400s
t=600s
t=800s
a
0.0 0.2 0.4 0.6 0.8 1.0 1.2 1.4 1.6
y [m]
vx [m/s]
S1
S2
S3
S4
S5
b
y [m]
0.3
0.2
0.1
0.0
-0.1
-0.2
-0.3
-0.4
-0.5
vy [m/s]
t=200s
t=400s
t=600s
t=800s
c
x [m]
0.2
0.1
0.0
-0.1
-0.2
-0.3
-0.4
vy [m/s]
S1
S2
S3
S4
S5
d
x [m]

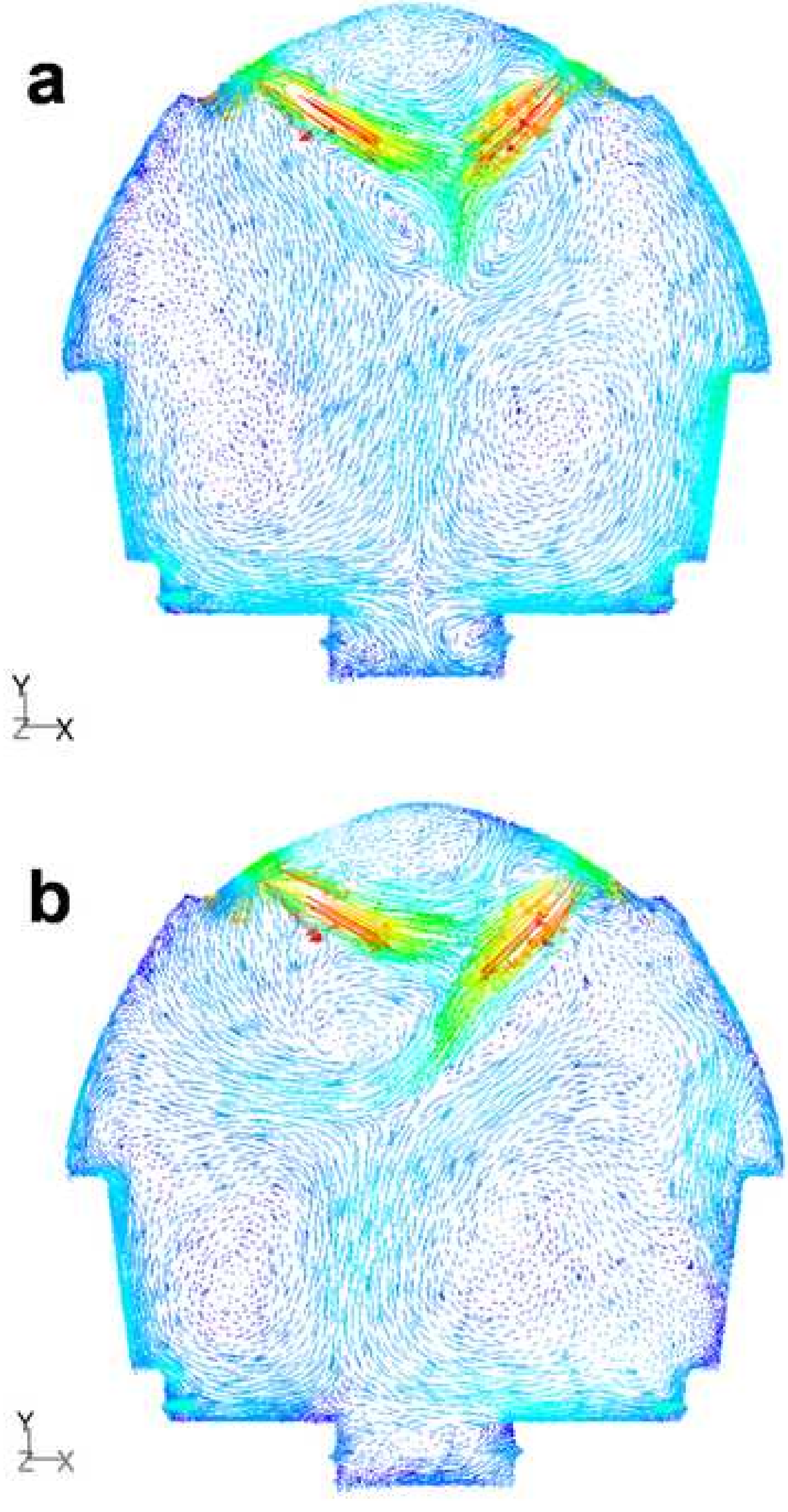
a
Y
Z
X
b
Y
Z
X